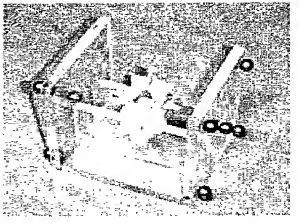

Fig. 1. Phantom containing cadaveric lumbar (L4) vertebra, constructed to allow registration of CT images, its triangulated surface representation, and ultrasonic images

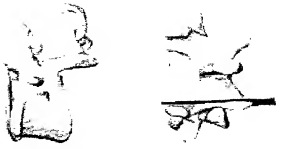

Fig. 2. Approximate planes for the images of the next figures overlayed on a rendering of the triangulated model for the vertebral surface. The plane for the transverse process images is shown on the left, and the plane for the lamina image is shown on the right

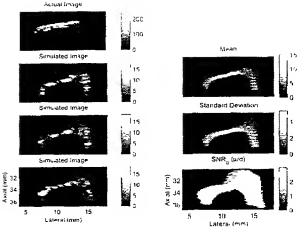

Fig. 4. Actual (top left) and three simulated images (bottom left) of the transverse process with corresponding statistical images (right). The images show only the small, approximately 6 mm axially and 15 mm laterally, portion of the entire image that represents scattering from the transverse process. The statistical images show the variation of the mean, standard deviation and SNR_0 across the image. The simulated images were generated for three different realizations of the microstructure, while the statistical images were computed directly from the model to characterize all possible images.

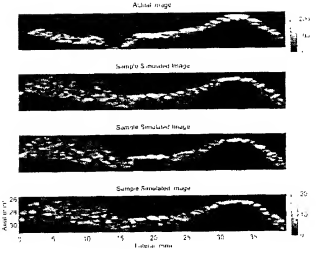

Fig. 4. Sample simulated images of the lamina and articular processes along with actual image of approximately the same region. From left to right, anatomical structures are the facet joint on the left (Rayleigh scattering with wide axial extent), the lamina in the center (non-Rayleigh scattering with relatively high amplitude) and the inferior articular process on the right (mix of Rayleigh on the sides and non-Rayleigh at the peak).

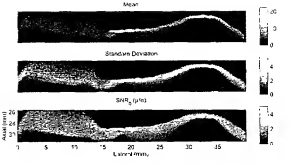

Fig. 5. Statistical images for the lamina and articular processes. Regions of non-Rayleigh scattering exist along the lamina and the peak of the articular process, although the lamina represents a site of greater SNR$_0$ than the articular process.

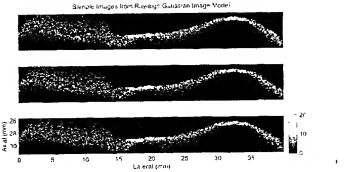

Fig. 6 Samples of a Rayleigh/Gaussian image model, with pixel intensities generated using the computations of previous sections are shown for the lamina image plane.